APPENDIX B

DETERMINATION OF DIFFUSION COEFFICIENTS IN POLYPYRROLE THIN FILMS USING A CURRENT PULSE RELAXATION METHOD

Determination of Diffusion Coefficients in Polypyrrole Thin Films Using a Current Pulse Relaxation Method

Reginald M. Penner**[1], Leon S. Van Dyke**, and Charles R. Martin*

Department of Chemistry

Texas A&M University

*Electrochemical Society Active member, to whom correspondance should be addressed.

**Electrochemical Society Student member.

[1]Present Address: Department of Chemistry, Stanford University, Stanford, CA 94305

Introduction

Diffusion coefficients for mobile species in electronically conductive polyheterocycles have been reported by several groups (1-5). In each case, a large amplitude electrochemical experiment such as potential step chronocoulometry (6) ~~has been~~ employed. Techniques like these based on the Cottrell Equation have been used previously to measure apparent diffusion coefficients in nonelectronically conductive redox polymer films (cf. 7-10). Unfortunately, an inherent problem with the application of large amplitude electrochemical methods to electronically conductive polymers is that of background correction. Feldburg (11) has shown that the charge associated with switching a conducting polymer between conducting and insulating redox states (as required by any large amplitude experiment) has a large capacitive component which is inseparable from the faradaic charge. That is, there is no simple method for correcting the experimentally observed signal (usually Q(t) or i(t)) for capacitive contributions. In the absense of a capacitance correction, the Cottrell Equation cannot yield accurate diffusion coefficient information (6). Moreover, this same problem exists for other large amplitude experiments such as cyclic voltammetry, differential pulse voltammetry, and chronopotentiometry.

A small amplitude electrochemical experiment, however, can circumvent the background correction problem since diffusion coefficient information can be gleened from an experiment in which the conducting polymer remains in the reduced (nonconducting) state. Under these circumstances, the relatively small capacitive contributions to the electrochemical signal can easily be estimated and compensated. Such a small amplitude current pulse experiment has been developed by Steele and coworkers (12) and by Worrell

and coworkers (13-16) to measure diffusion coefficients for intercalated species in alkali metal intercalation compounds. Using a more rigorous mathematical treatment of this experiment, we have developed a modification of the current pulse method suitable for thin, redox film-modified electrode systems. In addition to solving problems associated with background correction, the current pulse - E_{oc} relaxation method presented here has a number of other advantages for the determination of diffusion coefficients in thin films.

Here we describe this new method and its application to the determination of diffusion coefficients in electrochemically synthesized polypyrrole thin films. Diffusion coefficients for such films in Et_4NBF_4, MeCN are determined for a series of submicron film thicknesses. In addition, we report measurments of the double-layer capacitance, C_{dl}, and the resistance, R_u, of polypyrrole thin films as a function of potential obtained with the galvanostatic pulse method. Measurments of the electrolyte concentration in reduced polypyrrole films are also presented to aid in the interpretation of these data.

Theory

Previous current pulse - E_{oc} relaxation experiments - As noted above, a small amplitude, current pulse experiment was first used by Steele and coworkers (12) and by Worrell and coworkers (13-16) to measure diffusion coefficients for alkali metal atoms in layers of the intercalation compounds TaS_2, TiS_2 and TiO_2. The application of this technique to diffusion coefficient determinations in alkali metal intercalation compounds is now well established (17,18). In a typical experiment, a current pulse of some

duration, τ, and amplitude, i_p, is used to inject the diffusing species (usually Li^o or Na^o) at the electrolyte/film (electrode)interface. At the termination of the current pulse, the working electrode is returned to open circuit and its potential, E_{oc}, is monitored as a function of time. The perturbation in the concentration of the electroactive species at the electrode surface results in a displacement of E_{oc} as predicted by the Nernst equation (6):

$$E_{oc} = E^o_{ox/red} + (RT/nF)\ \ln([ox]_{x=0}/[red]_{x=0}) \qquad [1]$$

ie. E_{oc} is determined by the ratio [ox]/[red] at the electrode surface. At the termination of the current pulse ($t = \tau$), the electrochemically generated diffusion layer has a narrow distance distribution and the maximum potential excursion, $\Delta E_{oc} = |E_{oc,initial} - E_{oc,t}|$, is observed. At successively longer times, t, after the termination of the current pulse, the concentration of diffusing species at the electrode surface, $C_{diff,x=0}$, and ΔE_{oc} decrease as the diffusion layer relaxes into the bulk of the film. Since the rate at which the film reequilibrates is dependent on the diffusion coefficient, D_{diff}, of the intercalated species, D_{diff} can be determined from the experimentally observed rate at which ΔE_{oc} relaxes to $E_{oc,initial}$. In all systems studied to date, the rate of E_{oc} relaxation is linear with $t^{-1/2}$, and D_{diff} is extracted from the slope of this plot (12-16).

In the application of the current pulse - E_{oc} relaxation technique to alkali metal intercalation compounds, several assumptions are made which simplify the mathematical treatment of the experiment. These assumptions

are as follows: i) diffusion of the intercalated species is semi-infinite linear from the film/electrolyte interface. This assumption imposes an experimental constraint on the maximum duration of the experiment (6):

$$t_{max} < l^2/2D \qquad [2]$$

where l = film thickness, and t_{max} = time at which diffusion layer reaches film/electrolyte interface (maximum total experiment duration), ii) the equilibrium concentration of the injected species is not significantly perturbed by the quantity of diffusing species introduced by the current pulse, and, iii) the initial distribution of diffusing species existing at the termination of the current pulse is infinitely narrow, ie the diffusing species is initially dispersed in a plane at x=0 (19). If these assumptions are valid, the time dependence of ΔE_{oc} is given by (13,14,19):

$$\Delta E_{oc} = \frac{mi_p t}{FA(\ Dt)^{1/2}} \qquad [3]$$

where t is the time after the termination of the current pulse, and m is the slope of the linear E_{oc} vs. C_{diff} relation.

Assumption (i) limits the time window available for obtaining linear E_{oc} vs. $t^{-1/2}$ behavior consistant with Eq. 3 for any film thickness. Diffusion coefficients of 1 x 10^{-8} cm^2 sec^{-1} (Li_yTaS_2 (13)) and layer thicknesses, l = 50 μm, which are typical parameters for alkali metal intercalation compounds, correspond to t_{max} values (Eq. 2) of ca. 1000 sec. Experimentally, linear E_{oc} vs. $t^{-1/2}$ behavior is routinely observed for t < ca. 100 sec (12-15).

Although the diffusion coefficients measured for polypyrrole films are similar, much thinner films are required ($l < 1$ μm). The corresponding t_{max} value for such films is ca. 0.5 sec or less. Figure 1 shows the ΔE_{oc} vs. $t^{-1/2}$ plots obtained at several pulse current amplitudes for a typical 0.54 μm polypyrrole film. Note that as expected, ΔE_{oc} is not linear with $t^{-1/2}$ indicating that the simple, limiting behavior described by Eq. 3 is not observed for this system.

Calculation of $C_{diff,x=0}$ vs. time transients - Application of the current pulse - E_{oc} relaxation experiment to the measurement of diffusion coefficients in thin ($l < 1.0$ μm) films requires that an expression for ΔE_{oc} vs. t be derived which is free of the constraints imposed by assumptions (i) - (iv) above. We have accomplished this by calculating ΔE_{oc} vs. time transients with an expression which describes finite diffusion from a known initial distribution of diffusing species (that generated by the current pulse). The $C_{diff,x=0}$ vs. time transients generated from this more rigorous expression are converted to E_{oc} vs. time transients using calibration curve as described below. Since a simple $t^{-1/2}$ dependance is not observed for the resulting transients, diffusion coefficients are obtained by fitting the simulated E_{oc} vs. time transients to experimentally obtained transients.

Generation of simulated $C_{diff,x=0}$ vs. time transients for the current pulse experiment involves two discrete calculations. First, the initial concentration-distance profile of diffusing species must be calculated from the experimental current pulse parameters. This initial distribution is then used to calculate $C_{diff,x=0}$ for times after the termination of the

current pulse.

The equation describing linear diffusion for any initial distribution of diffusing species, f(x)', and finite geometry is given by (19):

$$C(x,t) = \frac{1}{l}\int_0^l f(x')dx' + \frac{2}{l}\sum_{n=1}^{\infty}\exp\left(\frac{-Dn^2\pi^2 t}{l^2}\right)\cos\left(\frac{n\pi x}{l}\right)\int_0^l f(x')\cos\left(\frac{n\pi x'}{l}\right)dx' \quad [4]$$

where x is the distance from the planar source (electrode), C(x,t) is the concentration of diffusing species at any x and $t > \tau$, t is the time after the termination of the current pulse, and l is the film thickness. $C_{diff,x=0}$ is obtained by solving Eq. 4 for x=0 the appropriate initial distribution of diffusing species. The expression which we have employed for f(x)' is that for a continuous planar source of diffusing species in semi-infinite geometry (20):

$$C(x',t) = \frac{i}{nF}\sqrt{\frac{t}{\pi D}}\exp\left(\frac{x^2}{4Dt}\right) - \frac{ix}{2nFD}erfc\left(\frac{x}{2\sqrt{Dt}}\right) \quad [5]$$

where τ is the current pulse duration, C(x',τ) is the concentration - distance profile (initial distribution) at $t = \tau$, and i is the current pulse amplitude. Note that Eq. 5 treats the semi-infinite case. Consequently, an experimental constraint is imposed on the maximum pulse duration, τ_{max}, which is the same as that given by Eq. 2 above. This constraint is much less serious that that associated with Eq. 3 since the current pulse duration is easily confined to acceptible values. For example, if D and l are taken to be 1 x 10^{-8} cm^2 sec^{-1} and 0.5 μm, respectively, the maximum allowable pulse duration (Eq. 2) is ca. 100 msec. With this provision, substitution of Eq. 5 into Eq. 4 yields an exact expression for $C_{diff,x=0}$

for any desired combination of experimental parameters.

Eqs. 4 & 5 assume that the diffusion coefficient of the thin film is uniform. $C_{diff,x=0}$ vs. time transients were also calculated which consider linear variations (increases) of the D_{diff} with increasing distance from the planar source. This was accomplished by assigning a diffusion coefficient, Dx, consistant with the desired gradient to every distance increment $x + \Delta x$ for which the numerical integration was performed. The initial distribution was then calculated using Eq. 5 exactly as before. The resulting initial distribution accounts rigorously for the existance of the diffusion coefficient gradient. The C_{diff} vs. x relation so obtained is then substituted into Eq. 4 where each time increment, $t + \Delta t$, was assigned an effective diffusion coefficient, $D_{eff,t}$. The value of Deff,t at each time increment $t + \Delta t$ was the average of the diffusion coefficient at the electrode surface, D_{min}, and D_x at a distance equal to the excursion of the diffusion layer, $D_{x,diff}$. Thus, the $D_{eff,t}$ value operative for some time interval $t + \Delta t$ is given by the equation:

$$D_{eff,t} = (2D_{min} + ((2Dt)^{1/2})D_{grad}))/\ 2$$
$$= (2D_{min} + D_{x,diff})/2 \qquad [6]$$

where $(2Dt)^{1/2}$ is the approximate diffusion layer thickness, D_{min} is the minimum diffusion coefficient at $x = 0$, and D_{grad} is the gradient of the diffusion coefficient with distance, x, from the planar source. This modification to Eq. 5 assumes that at each time interval $t + \Delta t$, $D_{eff,t}$ is uniform over the entire diffusion layer thickness.

Experimental

Materials and equipment - Platinum disk electrodes (r = 1.15 mm) were constructed and pretreated as described previously (21). Tin oxide coated glass OTE's (area = 15 cm^2) were used to prepare large area polypyrrole films suitable for conductivity measurements. These electrodes were cleaned in concentrated H_2SO_4 prior to use. Tetraethylammonium tetrafluoroborate (99%, Aldrich) was recrystallized from methanol and dried envacuo at 100 C for ca. 24 hrs. prior to use. Pyrrole (99%, Aldrich) was distilled under an inert atmosphere immediately prior to use. Acetonitrile (UV grade, Burdick & Jackson) was used as recieved. All solutions employed for electrochemical measurements were purged with purified N_2 prior to use.

The glass cells employed for all electrochemical measurements were of a conventional one compartment design. A large area, Pt gauze counter electrode (25 x 25 mm, AESAR) and a conventional saturated calomel reference electrode (SCE) were used for all electrochemical experiments.

Conductivity measurements were accomplished with a Yellow Springs Instruments Model 31 AC conductivity bridge and a YSI Model 3402 cell (cell constant = 0.1 ohm cm^{-1}).

Film deposition - Polypyrrole films were deposited from monomer solutions containing 0.5 M pyrrole in 0.2 M Et_4NBF_4, acetonitrile. Polymer deposition was accomplished galvanostatically using a EG&G Princeton Applied Research Model 273 potentiostat/galvanostat. A polymerization current density of 1.0 mA cm^{-2} was used for all films. Reproducible steady state potentials of 0.84 V $\pm$ 0.01 V vs. SCE were observed during film deposition at this current density.

C-2

Polypyrrole films were prepared with the above procedure in a series of film thicknesses from 0.1 μm to ca. 1.6 μm. The film thickness was measured for dried, oxidized films using a Tencor Alpha Step profilometer. As shown in Figure 2, the relationship between polymerization charge and film thickness is linear for polypyrrole films over this interval. The slope of the plot in Figure 2 is 37.8 mC · 0.1 μm^{-1}; substantially greater than the 24 mC · 0.1 μm^{-1} observed previously for polypyrrole-BF_4^- films prepared by Diaz et al (22). This calibration curve was used to prepare polypyrrole films of known thicknesses as described above. After film deposition, polypyrrole modified electrodes were transfered to monomer free, 0.2 M Et_4NBF_4, MeCN electrolyte and a cyclic voltammogram was recorded to ascertain the film quality. All subsequent electrochemical measurements were performed in this electrolyte.

Current step R_u and C_{dl} measurements - 0.27 μm thick polypyrrole films were used for the measurement of R_u and C_{dl}. R_u and C_{dl} information were obtained at open circuit potentials from -0.6 V to 0.4 V vs. SCE using the galvanostatic pulse method as described previously for polyacetylene films (23). In the present case, a train of four current pulses were generated with an IBM PC XT computer and applied with the PAR Model 273 potentiostat/galvannostat. Current pulses had durations of 1 msec and magnitudes of 290 $\mu A\ cm^{-2}$, 585 $\mu A\ cm^{-2}$, 875 $\mu A\ cm^{-2}$, and 1.17 $mA\ cm^{-2}$. Adjacent current pulses were separated by open circuit intervals of ca. 50 msec. The rise-time observed for the PAR Model 273 was < 2 μsec. Potential transients at $t \leq 100$ μsec were recorded with a Nicollet Model 2090 digital storage oscilloscope.

Prior to the application of the current pulse train, polypyrrole films were potentiostated at the desired potential for 120 sec, then allowed to equilibrate at open circuit until no potential drift was observed. The resulting R_u and C_{dl} data obtained at a series of potentials exhibited no significant hysteresis with varying potential. This indicates that the pretreatment procedure employed resulted in films which were essentially equilibrilibrated at the terminal open circuit potential. At each potential, the values of R_u and C_{dl} were obtained from plots of iR and dE/dt vs. i_p, respectively, as described below.

Film electrolyte concentration mesurements - 0.5 μm polypyrrole films were deposited on 15 cm^2 SnO_2 - glass electrodes as above. Freshly deposited films were then transfered to 0.2 M Et_4NBF_4, MECN electrolyte and reduced potentiostatically at -0.8 V for 10 minutes. During this time, the films changed from the characteristic black color of oxidized films to the characteristic yellow color of reduced polypyrrole. Three different procedures were then used to effect the extraction of the reduced films. "Unrinsed" films were transfered from the electrolyte solution directly to 100 ml pure MeCN in an electrolytic beaker where they were extracted for 20 h. "Dip-rinsed" films were removed from the electrolyte solution and quickly dipped into pure MeCN before extracting as above. "Long-rinsed" films were treated as per the dip-rinse procedure above except that film-covered electrodes were stirred in the MeCN rinse for ca. 10 sec prior to removal and extraction.

After the 20 h extraction period, the conductivity of the leaching solution was measured. A water bath was used to maintain a constant

temperature of 30 C for all conductivity measurments. The concentration of Et_4NBF_4 was determined from the conductivites observed for the leaching solutions by using a calibration curve constructed with Et_4NBF_4, MeCN solutions of known concentrations. The concentration of supporting electrolyte in the films was determined from the amount of measured electrolyte using a film volume of 7.5×10^{-4} cm^3.

Preparation of E_{OC} vs. [ppy^+] calibration curves - Determination of diffusion coefficients with the current pulse method necessitates converting the concentration of diffusing species at the electrode surface, $C_{diff,x=0}$, to E_{OC} values so that calculated and experimental data can be compared. In the case of electronically conductive polymers, the relationship between polymer oxidized sites, ppy^+, (or holes, h^+) and E_{OC} is required. In the present case, this relationship was established empirically using a procedure similar to the Electrochemical Voltage Spectroscopy (EVS) employed by Kaufman and coworkers to determine the % doping vs. E_{OC} relationship for polyacetylene (24-26).

The procedure used here was as follows. Freshly prepared 0.27 μm polypyrrole films were reduced potentiostatically at 1.0 V vs. SCE until currents decayed to ca. 100 nA cm^{-2}. Such films were assumed to be quantitatively reduced. A small quantity of anodic charge was then injected with a constant current pulse of 500 nA x 1 sec after which the working electrode was returned to open circuit. After allowing the electrode to equilibrate at open circuit for 20 sec., the terminal open circuit potential was recorded, a second charge injection performed, and the cycle repeated. This charge injection-equilibration cycle was repeated until the desired

terminal E_{oc} was acheived. In this way the $Q_{injected}$ vs. E_{oc} relationship can be determined for the potential interval of interest. The current modulation program for the collection of these data was controlled by the IBM PC XT using PAR Headstart electrochemical software and executed by the PAR MOdel 273. Excellent film to film reproducibility of the $Q_{injected}$ vs. E_{oc} calibration curves was obtained using this procedure. As discussed in detail below, the "raw" calibration data so obtained must be compensated for the effects of capacitance before the injected charge can be related to oxidized polymer equivalents.

Current pulse diffusion coefficient determinations - Current pulse induced E_{oc} transients were obtained by first reducing freshly synthesized, oxidized films at a potential of -0.8 V vs. SCE. Films were assumed to be quantitatively reduced at this potential when the observed current density decreased to ca. 500 nA cm^{-2}. The film was then potentiostated at an initial potential, $E_{initial}$ = -0.4 V. After allowing the current to decay again to < 500 nA cm-2, the working electrode was switched to open circuit and a 50 msec anodic current pulse of the desired amplitude (100 - 400 μA cm^{-2}) was applied. Current pulses were generated with a Princeton Applied Research Model 175 programmer and applied with a PAR Model 173 potentiostat/galvanostat. The resulting potential transients were recorded with the Nicollet Model 2090 oscilloscope. Note that after equilibration of the film at -0.4 V, virtually no drift in potential was observed upon switching to open circuit. Subsequent current pulse experiments at other current densities were performed by rereducing the film at -0.8 V and then reequilibrating at -0.4 V as before.

Calculation of simulated Eoc vs. time transients - Programs for generating simulated ΔE_{oc} vs. time transients were written in PASCAL (Turbo Pascal, Borland) and executed on a Compaq Portable II computer. Simulated and experimental data were compared using LOTUS 123 (Lotus Development) graphics. Curve fitting of the simulated transients to the experimental data was accomplished manually.

Results and Discussion

Cyclic voltammetry of polypyrrole films - A typical cyclic voltammogram at 20 mV sec^{-1} for a 0.27 μm polypyrrole film in 0.2 M Et_4NBF_4, MeCN is shown in Figure 3. Cyclic voltammograms for thicker films such as those used for diffusion coefficient measurements were qualitatively similar. As noted above, cyclic voltammograms were routinely used to ascertain the uniformity of freshly synthesized films prior to performing other electrochemical measurements.

C_{dl} and R_u determinations - Our primary purpose for conducting the galvannostatic pulse experiments was to obtain the C_{dl} vs. E_{oc} data required to correct $Q_{injected}$ vs. E_{oc} calibration curves for capacitive charge contributions. Thus, C_{dl} vs. E_{oc} data for potentials $E_{oc} < -0.3$ V were required. However, current pulse experiments were conducted over the entire potential interval from -0.6 V to 0.4 V so that the C_{dl} and R_u data so obtained could be compared with that previously obtained from the AC impedance analyses of polypyrrole thin films (21).

The galvannostatic pulse method has previously been used to obtained R_u

and C_{dl} information for electronically conductive polyacetylene films by Will (23). At very short times (t < 100 μsec) after the application of the current step, the potential response is approximated by that for a series RC circuit (6,23):

$$E = i_p(R_u + t/C_{dl}) \qquad [6]$$

Where R^u is the total series resistance of the circuit and C_{dl} is the double layer capacitance. The displacement of the potential immediatly after the application of the current pulse (t < 5 msec) is equal to ipRu (6). A linear increase of the potential with time is observed at longer times (5 msec < t < 100 msec) since this current is primarily that associated with the charging of the electrical double-layer (6).

Typical E vs. t transients for a 0.27 μm polypyrrole film are shown in Figure 4a. The line indicated for each plot is the linear regression fit of the data in the interval 20 μsec < t < 100 μsec. dE/dt values obtained from the slopes of these lines were plotted vs. the current pulse amplitude (Fig. 4b) and Cdl was calculated from the slope using the Eq. 6 (6,23). Values for the total uncompensated resistance of the system, R_u, were obtained from plots of iR_u (measured at 20 μsec) vs. i_{step} (Fig. 4b)(6).

Figure 5 shows the resulting C_{dl} and R_u values obtained from current pulse measurments at open circuit potentials from -0.6 to +0.4 V. The resistance of ca. 6 ohms observed for the oxidized conducting film is approximately that expected from the electrolyte resistance alone (21). Thus, resistance in excess of this value can be attributed to the polypyrrole film. C_{dl} values obtained at potentials E_{oc} < -0.4 V of 20 - 30

$\mu F\ cm^{-2}$ are similar to those observed for bare platinum electrodes in this electrolyte. Thus, at potentials were polypyrrole is not electronically conductive, the capacitance is approximately that derived from the charging of the platinum substrate surface only. At potentials $E_{oc} > -0.2$ V, C_{dl} reaches a maximum of ca. $2.5 \times 10^{-4}\ F\ cm^{-2}$ of geometric electrode area. This corresponds to a capacitance per unit volume of ca. $9\ F\ cm^{-3}$. This value is approximately an order of magnitude smaller than that obtained from cyclic voltammetry (27) and AC impedance measurements (21,28). This disparity is probably due to a nonuniform a current density distribution for the porous, electronically conductive film. At the short times accessed in this experiment, the current density is likely to be supported preferentially by double-layer charging of the exterior surfaces of the film. Consequently, the C_{dl} values observed for oxidized polymer with the current pulse method may approximate the capacitance of film/electrolyte interface. If this is the case, the C_{dl} value for the oxidized polymer obtained here tranlates to a roughness factor, R, (actual surface area/geometric surface area) of ca. 10 assuming the specific capacitance of the polymer is similar to that of platinum, $20\ \mu F\ cm^{-2}$. This R value seems reasonable considering the rough surface topology of electrochemically synthesized polypyrrole films.

Reduced, nonelectronically conductive films should not exhibit this effect, and C_{dl} values obtained at potentials, Eoc < -0.3 V ought to accurately reflect the total C_{dl} of the system. We have used these data to correct the $Q_{injected}$ vs. E_{oc} calibration data for capacitive contributions as discussed below. Note that accurate C_{dl} values are not obtained at potentials from -0.3 - -0.4 V by either cyclic voltammetry or AC impedance

since the currents measured by both methods at these potentials contain a significant faradaic component (21,29).

The variation of C_{dl} and R_u with potential shown in Figure 5 parallels the C_{dl} and R_u vs. E_{oc} data obtained previously from the AC impedance analyses of thin polypyrrole films (21). As the potential of the film is increased from -0.6 V, a sharp decrease in R_u is observed at potentials from -0.5 V to -0.3 V; at potentials negative of the transition in C_{dl}. Decreases in R_u at these potentials may reflect increases in either the ionic or the electronic conductivity of the electrochemical circuit (polymer film + electrolyte). However, C_{dl} scales with the electronic conductivity of the polymer film only. Thus, decreases in R_u in the absence of commensurate increases in C_{dl}, as observed for the polypyrrole/BF_4^- films here, must be the result of decreases in the ionic conductivity of the film. The data shown in Figure 5 suggests that at potentials of ca. -0.4 V, polypyrrole films possess high ionic conductivity but are relatively nonelectronically conductive. The origin of this effect is discussed below.

Measurement of the electrolyte concentration in ppy^O films - We have estimated the concentration of free electrolyte in reduced polypyrrole (ppy^O) films by extracting electrochemically reduced films in pure acetonitrile and measuring the conductivity of the leaching solution as described above. This information is important to the interpretation of the transport data obtained using the current pulse - E_{oc} relaxation technique described below. In addition, these data provide insight to the mechanism responsible for the transition in R_u at very negative potentials.

Film electrolyte concentrations as measured for 0.5 μm polypyrrole

films using unrinsed, dip-rinsed, and long-rinsed extraction techniques are listed in Table I. The precision of the data obtained for unrinsed films was low due to the fact that variable quantities of electrolyte adhered to the electrode as it was withdrawn from the electrolyte solution. This excess electrolyte was transfered to the leaching solution resulting in conductivity values and film electrolyte concentrations which we believe are anomolously high.

Good precision was obtained by dip-rinsing the polypyrrole films prior to extraction, as described above. The film electrolyte concentration of 5.4 M ± 0.5 M obtained using this procedure is surprisingly high considering the resistivity observed for such films. Note that reduced films were potentiostated at -0.8 V prior to dip-rinsing and extraction. This potential is well negative of the increase in R_u observed at -0.3 V - -0.5 V (Figure 5). These data suggest that the mobility of the electrolyte in the polymer at potentials E_{oc} < -0.3 V is limited, possibly due to a transport-restrictive morphology assumed by the polymer at these potentials. In this case, the increase in R_u shown in Figure 5 could be effected by morphological changes in the polymer which increase the film electrolyte mobility.

As shown in Table I, long-rinsed films (duration ca. 10 sec) yielded smaller film electrolyte concentrations. Some extraction of electrolyte from the film during the pre-rinse is inevitable with this procedure. Consequently, the electrolyte concentrations estimated with the long-rinse procedure are undoubtedly too low. However, the concentration values observed for long-rinsed films of ca. 2.85 M seem to suggest that removal of excess electrolyte is accomplished reliably with the faster, dip-rinse

procedure.

Preparation of [ppy$^+$] vs. E_{oc} calibration curves - The procedure for calculating E_{oc} relaxation transients necessitates converting the $C_{diff,x=0}$ values obtained from Eqs. 4 & 5 to E_{oc} values so that calculated and experimental data can be compared. This can be accomplished for a conventional redox couple simply by using the Nernst equation (Eq. 1). However, electronically conductive polymers may not conform strictly to the Nernst equation. Our approach has been to construct an empirical calibration curve by experimentally relating C_{ppy+} to E_{oc}. A similar procedure has been used to relate C_{Li} or C_{Na} to E_{oc} in alkali metal intercalation compound films (12-16).

The preparation of raw $Q_{injected}$ vs. E_{oc} calibration curves (or coulometric titration curves (29)) is discussed in detail above. One such curve for the potential interval from -0.3 V to -0.4 V is shown in Figure 6a. Note that current pulse - Eoc relaxation experiments were confined to this potential interval. $Q_{injected}$ values cannot be directly converted to chemical equivalents without first correcting for capacitive contributions. We have used C_{dl} values obtained from the current pulse experiments to subtract capacitive charge contributions from $Q_{injected}$. The resulting charge values corrected for capacitance, Q_{corr}, are plotted with $Q_{injected}$ in Figure 6a. Qcorr values were then converted to concentrations of oxidized polymer sites, C_{ppy}^+, assuming n = 1 eq mole^{-1}. A typical corrected calibration curve and the 4th order polynomial least squares fit to these data are shown in Figure 6b. Note that C_{ppy+} is calculated for a film thickness of 0.27 μm. The equation for the polynomial best fit was

subsequently used to convert calculated C_{ppy+} values to E_{oc} values for comparison to experimentally obtained data.

Interpretation of diffusion coefficients for polypyrrole - The open circuit potential observed for a polypyrrole film is determined by the concentration of oxidized sites in the polymer. Thus, if ideal Nernstian behavior were observed for polypyrrole, the appropriate Nernst equation is analogous to Eq. 1:

$$E_{oc} = E^{o}_{ppy+/ppyo} + (RT/nF)\ \ln(C_{ppy+,x=0}/C_{ppyo,x=0}) \qquad [8]$$

ie. E_{oc} is determined by the concentration of oxidized polymer sites, $C_{ppy^+,x=0}$ (or holes, h^+) at the electrode surface. In the strictest sense, diffusion coefficients measured using the current pulse - E_{oc} relaxation technique are values for the diffusion of these electrochemically generated holes, h^+. However, it is commonly assumed that diffusion of these positively charged species is limited by that of electrostatically bound anions, in this case BF_4^-. Given the unexpectedly large concentrations of free electrolyte in reduced polypyrrole films reported above, the possibility also exists that anions and cations are relatively immobile species, and that the apparent diffusion coefficient is limited by the rate of electron-hopping between essentially stationary anionic sites. Alternatively, the measured diffusion coefficient may reflect contributions from both cation and anion diffusion. We are currently measuring diffusion coefficients for a large number of electrolytes in order to ascertain the relative importance of factors such as cation size and anion size in an

attempt to understand diffusion in these polymers more completely. In the present work, we have refered to all measured diffusion coefficient values as $D_{Et_4NBF_4}$ consistant with the previously established convention (1-5). However, it should be noted that the factors controlling the diffusion of electrochemically generated h^+ in the polyheterocycles have not as yet been elucidated.

Behavior of simulated E_{oc} vs. time transients - Simulated ΔE_{oc} vs. time transients were calculated using conventional numerical methods from Eqs. 4 & 5. The rate of the E_{oc} decay following the termination of the current pulse depends primarily on the film thickness, 1, and the diffusion coefficient, D_{diff} as shown in Eq. 5. Figure 7 shows simulated E_{oc} vs. time transients for a series of four diffusion coefficient values and experimental parameters similar to those encountered in the present study. These data show that for 1 = 0.5 μm, substantial differences in the E_{oc} relaxation rate exist for diffusion coefficients which differ by as little as 20%. Note that these E_{oc} relaxation transients occur on a convenient experimental time scale of ca. 1 sec.

The effect of film thickness on simulated ΔE_{oc} vs. time transients is shown in Figure 8. Both the rate of the E_{oc} relaxation and the value of the final equilibrium potential are noticably affected by changes in the film thickness of 20%. As shown in Eq. 5, the approximately exponential Eoc relaxtion rate is proportional to exp (1^{-2}). Thus, errors present in the measurement of the film thickness radically affect the accuracy of the diffusion coefficients calculated with this technique.

Simulated ΔE_{oc} vs. time transients can also be generated for films in

which the diffusion coefficient is nonuniform using the procedure outlined above. Such transients were calculated assuming a linear gradient of the diffusion coefficient, D_{grad}, with film thickness for comparison with the experimental ΔE_{OC} vs. time transients obtained for 0.73 mm and 0.95 mm films (see discussion below). The effect of D_{grad} on simulated ΔE_{OC} vs. time transients is shown in Figure 9. Note that the diffusion coefficient, D_{min}, at x=0 for each of the transients A-D was 1 x 10^{-9} cm^2 sec^{-1}. The rate of the observed E_{OC} relaxation rate increases with D_{grad} as expected. However, in constrast to the behavior shown in Figure 7, the maximum excursion in E_{OC} observed at short times is similar for all of the transients Fig. 9A - 9D.

Experimental Eoc vs. time transients for polypyrrole thin films - Diffusion coefficients were measured for polypyrrole films with thicknesses of 0.35 μm, 0.54 μm, 0.73 μm, and 0.95 μm. Polypyrrole films with thicknesses greater than ca. 1 μm cannot be quantitatively addressed electrochemically, ie. the as-synthesized oxidized films cannot be quantitively reduced (27,30). For this reason, films with thicknesses greater than 1 μm were not employed in this study.

Current pulse experiments were performed from an initial potential of -0.4 V vs. SCE. The maximum potential excursions observed for these experiments were approximately 50 mV. Thus, all current pulse - Eoc relaxation experiments were confined to potentials from -0.4 V to -0.35 V vs. SCE. Because this potential interval is well negative of the polymer E^o of -0.2 V, the polypyrrole film remained in its reduced, nonconducting redox state throughout the experiment. The fact that polypyrrole films at these potentials are essentially nonelectronically conductive is supported

by the capacitance data of the present paper (Figure 5) and by previous experimental evidence (21,31,32).

ΔE_{oc} vs. time transients were obtained for all films with current pulse amplitudes of 100, 200, 300, and 400 $\mu A\ cm^{-2}$, anodic. The quantity of charge injected during the current pulse, $Q_{injected}$, was corrected for capacitance. The capacitive component of $Q_{injected}$ was estimated from the C_{dl} data obtained from the current pulse experiments discussed above based on the maximum potential excursion observed during the application of the current pulse.

Simulated E_{oc} vs. time transients were fit to experimental transients for 0.35 μm and 0.54 μm polypyrrole films assuming the diffusion coefficient in these films was uniform. Excellent agreement between simulated and experimental transients was obtained at current pulse amplitudes of from 100 - 400 $\mu A\ cm^{-2}$ for films of either thicknesses. Typical simulated and experimental transients are shown in Figure 10 for a 0.5 μm film. The best fit diffusion coefficients obtained from these data are listed in Table II. Note that the variation in diffusion coefficient values observed over the range of current densities employed here was typically less than 10%. It is worth noting that the experimental parameters employed for these measurements are incompatible with the assumptions listed above for Eq. 3. For example, the overall redox state of the polypyrrole film is substantially altered for ip = 300 $\mu A\ cm^{-2}$ and 400 $\mu A\ cm^{-2}$ as evidenced by the terminal ΔE_{oc} values observed for equilibrated films. In addition, the excursion of the diffusion layer as calculated from Eq. 2 excedes the film thickness for both 0.35 μm and 0.54 mm film thicknesses ($t_{max} < 0.5$ sec) indicating that diffusion is effectively finite. Thus, the nonlinearity of

experimental ΔE_{oc} vs. $t^{-1/2}$ plots such as that shown in Fig. 1 is not surprising. However, these effects are taken fully into account by Eq. 4 & 5 as evidenced by the excellent fit obtained between experiment transients and those calculated from these equations.

It is important to note that the diffusion layer thickness at the termination of the current pulse does not equal the film thickness for pulse durations of 50 msec. For example, the 0.35 μm films prepared in this study which exhibited the fastest diffusion coefficients, t_{max} values calculated from Eq. 2 and the $D_{Et_4NBF_4}$ values listed in Table II are greater than 75 msec. Thus, diffusion during generation of the initial distribution is effectively semi-infinite and the experimental constraint imposed by Eq. 5 is satisfied.

The diffusion coefficient values measured for 0.35 μm and 0.54 μm thick films (Table II) are higher than the those for polypyrrole-BF_4^- thin films measured by Diaz and coworkers with chronoamperometry (34). We have previously reported $D_{Et_4NBF_4}$ values for polypyyrole films in Bu_4NBF_4, MeCN electrolyte using AC impedance methods. The values so obtained of ca. 1 x 10^{-9} cm^2 sec^{-1} are also significantly slower than observed here. Although it is tempting to attribute this latter disparity to the higher mobility of the Et_4N^+ cation as compared to Bu_4N^+, as noted above we are currently measuring $D_{Et_4NBF_4}$ values for a large number of electrolytes using both AC impedance and current pulse - E_{oc} relaxation methods in order to ascertain the origin of this effect. The difference in the diffusion coefficients obtained for the 0.35 μm film and the 0.54 μm film are reproducible. The origin of this effect is discussed in detail below.

Adaquate agreement between experimental and simulated E_{oc} vs. time

transients was obtained again assuming a uniform diffusion coefficient for films with thicknesses of 0.73 μm. However, experimentally observed ΔE_{oc} values at short times are greater by as much as 1 - 2 mV than the ΔE_{oc} values predicted by the best fit simulated data. In effect, a good fit of the simulated to the experimental data cannot be obtained for both the short time ΔE_{oc} data ($t < 0.1$ sec) and the data obtained at longer times. This is shown in Figure 11a where an experimental ΔE_{oc} vs. time transient for a typical 0.73 mm film (i_p = 100 μA) is compared with simulated transients. Three simulated transients were calculated; the diffusion coefficient corresponding to curve A was that neccessary to achieve the ΔE_{oc} excursion observed at times $t < 0.1$ sec, curve B was calculated using a $D_{Et_4NBF_4}$ value appropriate for the long time data, $t > 0.1$ sec. These diffusion coefficients values are listed in Table II. Note that $D_{Et_4NBF_4}$, curve A is approximately a factor of two faster than $D_{Et_4NBF_4}$, curve B. These data suggest that the diffusion coefficient may vary (increase) with increasing distance from the substrate electrode in the polypyrrole film. In order to test the effect that such a gradient would have on the resulting ΔE_{oc} vs. time relaxation transients, simulated transients were calculated assuming a linear gradient of $D_{Et_4NBF_4}$ with film thickness. The calculation of such transients is described in the theory section above. Figure 11a, curve C shows the best fit to the experimental data obtained with this model. The diffusion coefficient at the electrode/film interface for curve C was 4.2×10^{-9} cm^2 sec^{-1} and that at the film electrolyte interface was 8×10^{-8} cm^2 sec^{-1}. Note that ΔE_{oc} at times, $t < 0.1$ sec is fit well with this model, and the fit to data for $t > 0.1$ sec is slightly worse than that obtained with a uniform $D_{Et_4NBF_4} = 7 \times 10^{-9}$ cm^2 sec^{-1}, (curve B).

Experimental ΔE_{oc} vs. time curves for the 0.95 μm thick polypyrrole films were analyzed using exactly the same procedure as that employed for the 0.73 μm films above. A typical ΔE_{oc} vs. time transient for such a film (ip = 100 μA) is shown in Figure 11b. Again, curves A and B represent the best fits of simulated data for uniform $D_{Et_4NBF_4}$ values to the short time and the long time regions of the experimental transient, respectively. For this thicker polypyrrole film, the disparity between either curve A or B and the experimental data is more pronounced than for the 0.73 μm films. The diffusion coefficients corresponding to these curves (Table II) differ by a fact of 2. Figure 11b shows that the uniform diffusion coefficient model is clearly inadequete to describe the experimental ΔE_{oc} vs. time transients. Figure 11b, curve C represents the best fit obtained considering a linear gradient of diffusion coefficients in the film. The initial, short time regions of the experimental data are very well accomodated, although the ΔE_{oc} decay at times $t > 0.2$ sec procedes at a slower rate than predicted by this model. Again, the D_{min} value corresponding to curve C is similar to that used to obtain curve A.

To summerize the data presented for 0.73 μm and 0.95 μm polypyrrole films, the existance of a linear diffusion coefficient gradient does not account perfectly for the observed ΔE_{oc} - time transients. However, significantly better agreement is obtained particularly for the short time data than is possible by assuming uniform diffusion coefficient values for these films. Consequently, it seems likely that some dependence of $D_{Et_4NBF_4}$ exists on the film thickness in these relatively thick films. As a result, $D_{Et_4NBF_4}$ values increase with film thickness from the electrode/film interface to the film edge. The origin of this effect, and that responsible

for the variation of $D_{Et_4NBF_4}$ observed over the entire thickness interval from 0.35 μm - 0.95 μm is discussed below.

The increases in $D_{Et_4NBF_4}$ with film thickness observed here suggests that a gradient in the morphology of polypyrrole may exist in these thin films. This conclusion is supported by the fact that a diffusion coefficient gradient can be invoked to improve the aggreement between simulated and experimental ΔE_{oc} - time transients obtained for thick (0.73 μm and 0.95 μm) films. We have previously observed inconsistancies in the AC impedance specta of polypyrrole thin films which also suggest the presence of such a morphology gradient (21). As noted in this previous paper, the electrochemical synthesis of polypyrrole may facilitate the introduction of such morphology "density" gradients since the polymerization reaction does not occur at diffusion control (34). As a result, the polymerization reaction can procede at interior surfaces of the polymer film as well as at the film edge. The greatest accumulation of electrochemically deposited polymer then occurs near the electrode surface where the longest total duration is available for polymerization. The effective pore diameter (and hence $D_{Et_4NBF_4}$) of the resulting film increases with distance from the substrate electrode.

Conclusion

In the most general sense, we present here a small amplitude, DC electrochemical method for measuring diffusion coefficients in redox polymer thin films. The advantages of the current pulse - E_{oc} relaxation method as compared to conventional large amplitude electrochemical techniques (eg. chronocoulometry) are as follows: i) the current amplitude, i_p, can be

adjusted to very small values limited only by instrumental constraints, ie. potential sensitivity. Consequently, E_{oc} excursions can easily be confined to $\Delta E_{oc} < 10$ mV. Thus, diffusion coefficient information can be obtained for any discrete ratio [ox]/[red] and characteristics of the system associated with a particular redox state can be elucidated, ii) diffusion coefficient information is obtained from an open circuit region of the experiment. The adverse effects of migration and iR drop, which can be particularly serious for film-modified electrodes, are minimized as a result, iii) the model for calculating ΔE_{oc} - time transient presented here considers the finite diffusion case. Unlike electrochemical techniques based on the Cottrell equation, it is unneccessary to achieve semi-infinite diffusion in order to obtain reliable diffusion coefficient information, and, iv) the numerical approach to calculating ΔE_{oc} - time transients facilitates modifications which take into consideration effects such as the diffusion coefficient - thickness gradient discussed *vida supra*.

It should be noted that the application of the current pulse - Eoc relaxation technique to redox polymer films will be simplified in many case since the construction of an empirial calibration curve will not be nessessary for systems which can be assumed to exhibit Nernstian behavior.

The AC impedance analysis of redox films previously reported by Ho et al (29) and Rubinstein et al (33) can evince similar advantages due to the small amplitude of the applied potential sine-wave. Since diffusion coefficient information for the AC impedance experiment is obtained at steady-state, this experiment ought to be considered complimentary to the DC current pulse - E_{oc} relaxation experiment.

We have reported diffusion coefficients for polypyrrole thin films at a

series of submicron film thicknesses. These data point to the existence of a diffusion coefficient gradient with distance from the electrode surface in the polypyrrole film. Such a gradient might be due to structural changes in the film such that the polymer morpholgy is dense (transport restrictive) at the electrode/film interface and relatively open at the film/electrolyte interface. Since the electrochemical syntheses of other electronically conducting polyheterocycles (eg. polythiophene) are similar to that for polypyrrole, this observation may prove to be a general one.

In addition, the current pulse measurments of C_{dl} and R_u vs. potential presented here corroborate data previously obtained by AC impedence analyses of polypyrrole thin films (21). The magnitude of the C_{dl} values measured for the oxidized polymer suggests that the current pulse technique yields C_{dl} values for the polymer/electrolyte interface only, ie. the capacitance of the film edge. Measurements of the electrolyte concentration in reduced polypyrrole films reveal that quantitatively reduced films contain unexpectedly large concentrations of free electrolyte. This information has important implications for the interpetation of the observed dependencies of C_{dl} and R_u on potential.

Credit

This work was suported by the Office of Naval Research, the Robert A. Welch Foundation, the Air Force Office of Scientific Research, and NASA.

References

1. E.M. Genies, G. Bidan, and A.F. Diaz, *J. Electroanal. Chem.*, **149**, 101 (1983).
2. P. Marque, J. Roncali, and F. Garnier, *J. Electroanal. Chem.*, **218**, 107 (1987).
3. G. Nagasubramanian, S. Di Stefano, and J. Moacanin, *J. Phys. Chem.*, **90**, 4447 (1986).
4. C. Chiba, T. Ohsaka, and N. Oyama, *J. Electroanal. Chem.*, **217**, 239 (1987).
5. N.S. Sundaresan, S. Basak, M. Ponerantz, and J.R. Reynolds, *J.C.S. Chem. Commun.*, In Press.
6. A.J. Bard and L.R. Faulkner, "Electrochemical Methods: Theory and Applications," John Wiley & Sons, New York, 1980, Chpts. 3,4.
7. P. Daum, J.R. Lenhard, D. Rolison, and R.W. Murray, *J. Am. Chem. Soc.*, **102**, 4649 (1980).
8. C.R. Martin and K.A. Dollard, *J. Electroanal. Chem.*, **159**, 127 (1983).
9. F.C. Anson, J.M. Saveant, and K. Shigehara, *J. Am. Chem. Soc.*, **105**, 1096 (1983).
10. D.A. Buttry and F.C. Anson, *J. Am. Chem. Soc.*, **105**, 685 (1983).
11. S.W. Feldburg, *J. Am. Chem. Soc.*, **106**, 4671 (1984).
12. D.A. Winn, J.M. Shemilt, and B.C.H. Steele, *Mat. Res. Bull.*, **11**, 559 (1976).
13. S. Basu and W.L. Worrell, in "Fast Ion Transport in Solids", P. Vashishta, J.N. Mundy, G,K. Shenoy, Editors, p. 149, Elsevier North Holland, Inc., Amsterdam (1979).

14. S. Basu and W.L. Worrell, "Proceedings of the Symposium on Electrode Materials and Process for Energy Conversion and Storage", J.D.E. McIntyre, S. Srinivasan and F.G. Will, Editors, p. 861, The Electrochemical Society, Princeton, NJ (1977).

15. A.S. Nagelburg and W.L. Worrell, ibid., p. 861 (1977).

16. A.S. Nagelburg and W.L. Worrell, p. 948, The Electrochemical Society Extended Abstracts, Vol 77-1, Philedelphia, Pennsylvannia (1977).

17. M. Ottaviani, S. Panero, S. Morzilli, B. Scrosati, and M Lazzari, *Solid State Ionics*, **20**, 197 (1986).

18. W. Weppner and R.A. Huggins, *Ann. Rev. Mater. Sci.*, **8**, 269 (1978).

19. J. Crank, "The Mathematics of Diffusion", Oxford University Press, London, 1956, Chapt. 2.

20. J.S. Carslow and J.C. Jaeger, "Conduction of Heat in Solids", Oxford University Press, London, 1959, Chapt. 10.

21. R.M. Penner and C.R. Martin, submitted to J. Electrochem. Soc.

22. A.F. Diaz and J.I. Castillo, *J.C.S. Chem. Commun.*, 397 (1980).

23. F.G. Will, *J. Electrochem. Soc.*, **132**, 2093 (1985).

24. J.H. Kaufman, J.W. Kaufer, A.J. Heeger, R. Kaner, and A.G. MacDiarmid, *Phys. Rev. B.* **26**, 2327 (1982).

25. J.H. Kaufman, T. -C. Chung, A.J. Heeger, *Solid State Comm.*, **47**, 585 (1983).

26. J.H. Kaufman, T.-C. Chung, A.J. Heeger, *J. Electrochem. Soc.*, **131**, 2847 (1984).

27. A.F. Diaz, J.I. Castillo, J.A. Logan, and W.-Y. Lee, *J. Electroanal. Chem.*, **129**, 115 (1981).

28. P. Burgemayer and R.W. Murray, *J. Am. Chem. Soc.*, **104**, 6139 (1982).

29. C. Ho, I.D. Raistrick, and R.A. Huggins, *J. Electrochem. Soc.*, 127, 343 (1980).

30. G.B. Street, T.C. Clarke, M. Krounbi, K. Kanazawa, V. Lee, P. Pfluger, J.C. Scott, and G. Wieser, *Mol. Cryst. Liq. Cryst.*, 83, 253 (1982).

31. G.R. Kittlesen, H.S. White, and M.S. Wrighton, *J. Am. Chem. Soc.*, 106, 7389 (1984).

32. B.J. Feldman, P. Burgemayer, and R.W. Murray, J. Am. Chem. Soc., 107, 872 (1985).

33. I. Rubinstein, J. Rishpon, and S. Gottesfeld, *J. Electrochem. Soc.*, 133, 729 (1986).

34. E.M. Genies, G. Bidan, and A.F. Diaz, *J. Electroanal. Chem.*, 149, 101 (1983).

Table I. Measurement of the Electrolyte Concentration in Reduced Polypyrrole Thin Films

Experimental Method	Concentration Leaching Solution[a] (M)	Concentration Film[b] (M)
Unrinsed	$1.68 \times 10^{-4} \pm 8.9 \times 10^{-5}$	22.2 ± 13.1
Dip-rinsed	$4.06 \times 10^{-5} \pm 3.8 \times 10^{-6}$	5.40 ± 0.50
Long-rinsed[c]	$2.15 \times 10^{-5} \pm 6.0 \times 10^{-7}$	2.86 ± 0.08

[a]Leaching solution concentrations determined from the AC conductivity of solution obtained after a ca. 20 h extraction of reduced films.

[b]Film electrolyte concentrations were calculated assuming a film volume of 7.5×10^{-4} cm^3.

[c]Two films only were measured using this procedure.

Table II. Diffusion Coefficients For Polypyrrole Thin Films

Film Thickness μm	$D_{Et_4NBF_4}$ at x=0 $\times 10^{-10}$ cm^2 sec^{-1}	$D_{Et_4NBF_4}$ at x=1 $\times 10^{-10}$ cm^2 sec^{-1}	$D_{Et_4NB_4}$ gradient $\times 10^{-4}$ cm sec^{-1}
0.35[a]	83 ± 3	same	0
0.54[a]	62 ± 3	same	0
0.73[b]	42 ± 5	800 ± 90	2.0 ± 0.5
0.95[b]	3.0 ± 0.4	290 ± 40	2.0 ± 0.5

[a]Diffusion coefficients correspond to the best fit of the experimental ΔE_{oc} relaxation transient to that predicted from Eqs. 4 & 5. The values reported are averages obtained for eight trials; two different films and four current densities each (100 - 400 μA cm^{-2}).

[b]Diffusion coefficients were calculated as above except that a linear gradient of diffusion coefficents is assumed to obtain over the film thickness as described *vida infra*. The values reported are the averages obtained for eight trials as above.

Figure Captions

Figure 1 - ΔEoc vs. $t^{-1/2}$ plots at a series of current pulse amplitudes for a 0.5 μm polypyrrole film in 0.2 M Et_4NBF_4, MeCN.
Einitial = -0.4 V, Current pulse amplitudes are: A - 400 $\mu A\ cm^{-2}$, B - 300 $\mu A\ cm^{-2}$, C - 200 $\mu A\ cm^{-2}$, and D - 100 $\mu A\ cm^{-2}$.

Figure 2 - Polymerization charge vs. film thickness calibration curve for polypyrrole films prepared galvanostatically at ip = 1.0 $mA\ cm^{-2}$ in 0.5 M pyrrole, 0.2 M Et_4NBF_4, MeCN.

Figure 3 - Cyclic voltammogram for a typical 0.27 μm polypyrrole film at 20 $mV\ sec^{-1}$ in 0.2 M Et_4NBF_4, MeCN supporting electrolyte.

Figure 4 - (a) Polarization vs. time transients for a 0.27 μm polypyrrole film at four pulse current densities. $E_{initial}$ = -0.375 V, current pulse amplitudes for these transients were (from top): 1.17 $mA\ cm^{-2}$, 875 $\mu A\ cm^{-2}$, 585 $\mu A\ cm^{-2}$, and 290 $\mu A\ cm^{-2}$.
(b) Plots of dE/dt (closed circles) and iR (open circles) vs. current pulse amplitude for the data shown in figure 4a.

Figure 5 - C_{dl} (closed circles) and R_u (open circles) vs. open circuit potential obtained using the galvanostatic pulse method for 0.27 μm thick polypyrrole films.

Figure 6 - (a) $Q_{injected}$ and Q_{corr} vs. E_{oc} raw calibration curve data for 0.27 μm polypyrrole films in 0.2 M Et_4NBF_4, MeCN. Q_{corr} values were obtained by subtracting the capacitive contributions to the injected charge using capacitance values obtained from the galvanostatic pulse measurements.
(b) E_{oc} vs. C_{ppy+} calibration curve caluculated from the Q_{corr} vs. E_{oc} data in figure 6a.

Figure 7 - Simulated ΔE_{oc} vs. time transients for four diffusion coefficient values calculated for the following experimental parameters: $l = 0.5\ \mu m$, $\tau = 50$ msec, and diffusion coefficient values of: A - 2×10^{-9} cm^2 sec^{-1}, B - 2.5×10^{-9} cm^2 sec^{-1}, C - 3×10^{-9} cm^2 sec^{-1}, and, D - 4×10^{-9} cm^2 sec^{-1}.

Figure 8 - Simulated ΔE_{oc} vs. time transients for four values of the film thickness calculated for the following experimental parameters: t = 50 msec, $D = 1 \times 10^{-9}$ cm^2 sec^{-1}, and film thicknesses of: A - 0.20 μm, B - 0.25 μm, C - 0.30 μm, and D, 0.50 μm.

Figure 9 - Simulated ΔE_{oc} vs. time transients for four gradients of the diffusion coefficient, D_{grad}, calculated for the following experimental parameters: $\tau = 50$ msec, $D_{min} = 1 \times 10\text{-}9$ cm^2 sec^{-1}, $i_p = 100\ \mu A\ cm^{-2}$, and D_{grad} values of: A - 0 (no gradient), B - 2×10^{-5} cm sec^{-1}, C - 6×10^{-5} cm sec^{-1}, and D - 1×10^{-4} cm sec^{-1}.

Figure 10 - Simulated and experimental ΔE_{oc} vs. time transients for a typical 0.5 μm polypyrrole film in 0.2 M Et_4NBF_4, MeCN. $E_{initial} = -0.4$ V, $\tau = 50$ msec. Current pulse densities, i_p and diffusion coefficients for the calculated transients were as follows: (a) - $i_p = 100\ \mu A$ cm-2, $D_{Et4NBF4} = 6.0 \times 10^{-9}$ cm^2 sec^{-1}, (b) - ip = 200 $\mu A\ cm^{-2}$, $D_{Et4NBF4} = 6.0 \times 10^{-9}$ cm^2 sec^{-1}, (c) - ip = 300 $\mu A\ cm^{-2}$, $D_{Et4NBF4} = 6.0 \times 10^{-9}$ cm^2 sec^{-1}, and (d) - ip = 400 $\mu A\ cm^{-2}$, $D_{Et4NBF4} = 6.5 \times 10^{-9}$ cm^2 sec^{-1},

Figure 11 - Calculated and experiment ΔE_{oc} vs. time transients for 0.73 μm and 0.95 μm polypyrrole films. $\tau = 50$ msec, $i_p = 100\ \mu A\ cm^{-2}$. (a) - $l = 0.73\ \mu m$, simulated transients were calculated using the following $D_{Et4NBF4}$ values: A - 4.0×10^{-9} cm^2 sec^{-1},

B - 7.0×10^{-9} cm^2 sec^{-1}, C - $D_{Et_4NBF_4}$ gradient with $D_{min} = 4.2 \times 10^{-9}$ cm^2 sec^{-1} and $D_{grad} = 1.5 \times 10^{-4}$ cm sec^{-1}.

(b) - l = 0.95 μm, simulated transients were calculated using the following $D_{Et_4NBF_4}$ values: A - 5.0×10^{-10} cm^2 sec^{-1}, B - 1.0×10^{-9} cm^2 sec^{-1}, C - $D_{Et_4NBF_4}$ gradient with $D_{min} = 3.0 \times 10^{-10}$ cm^2 sec^{-1} and $D_{grad} = 2.0 \times 10^{-4}$ cm sec^{-1}.

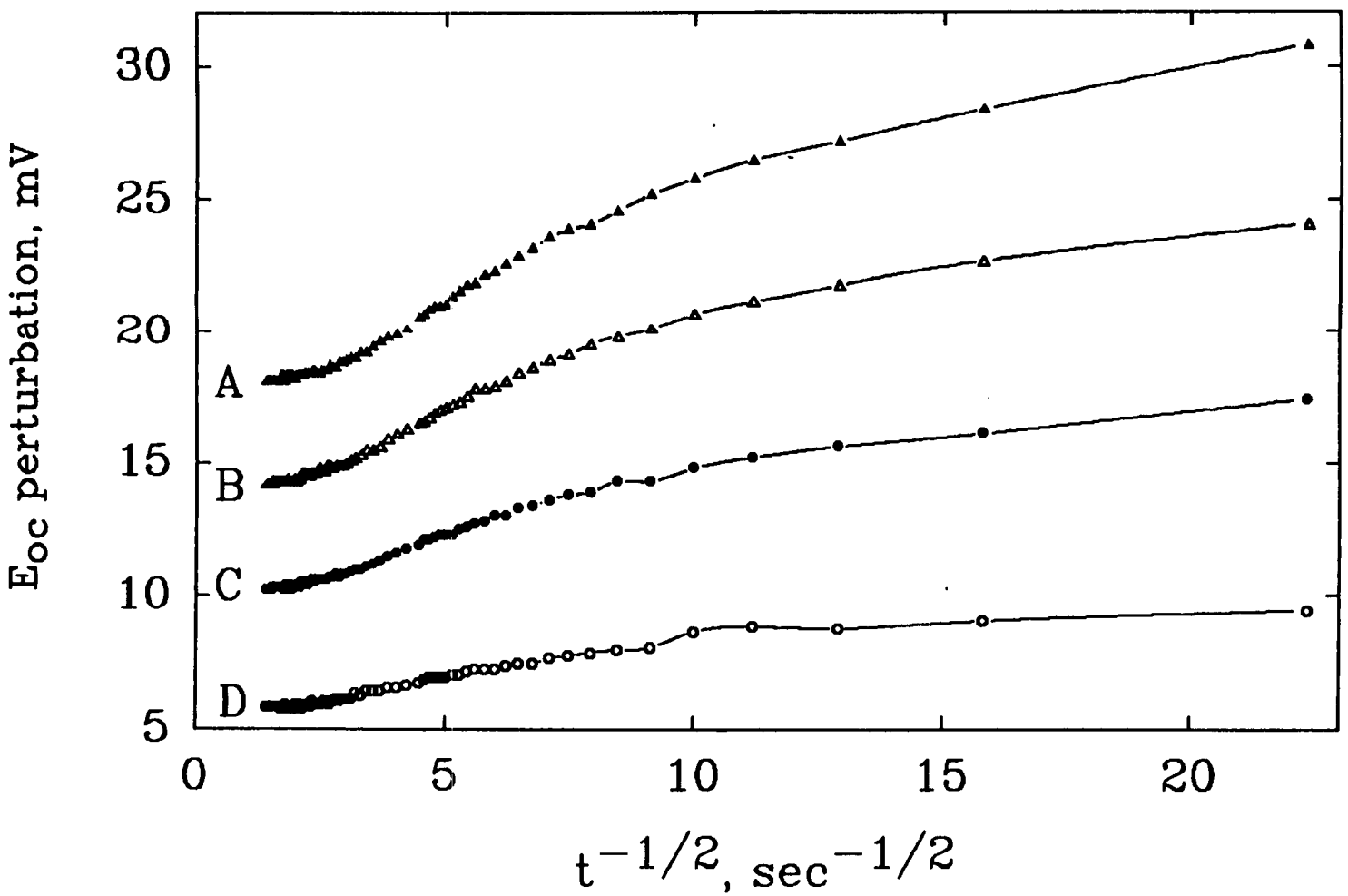

Figure 1

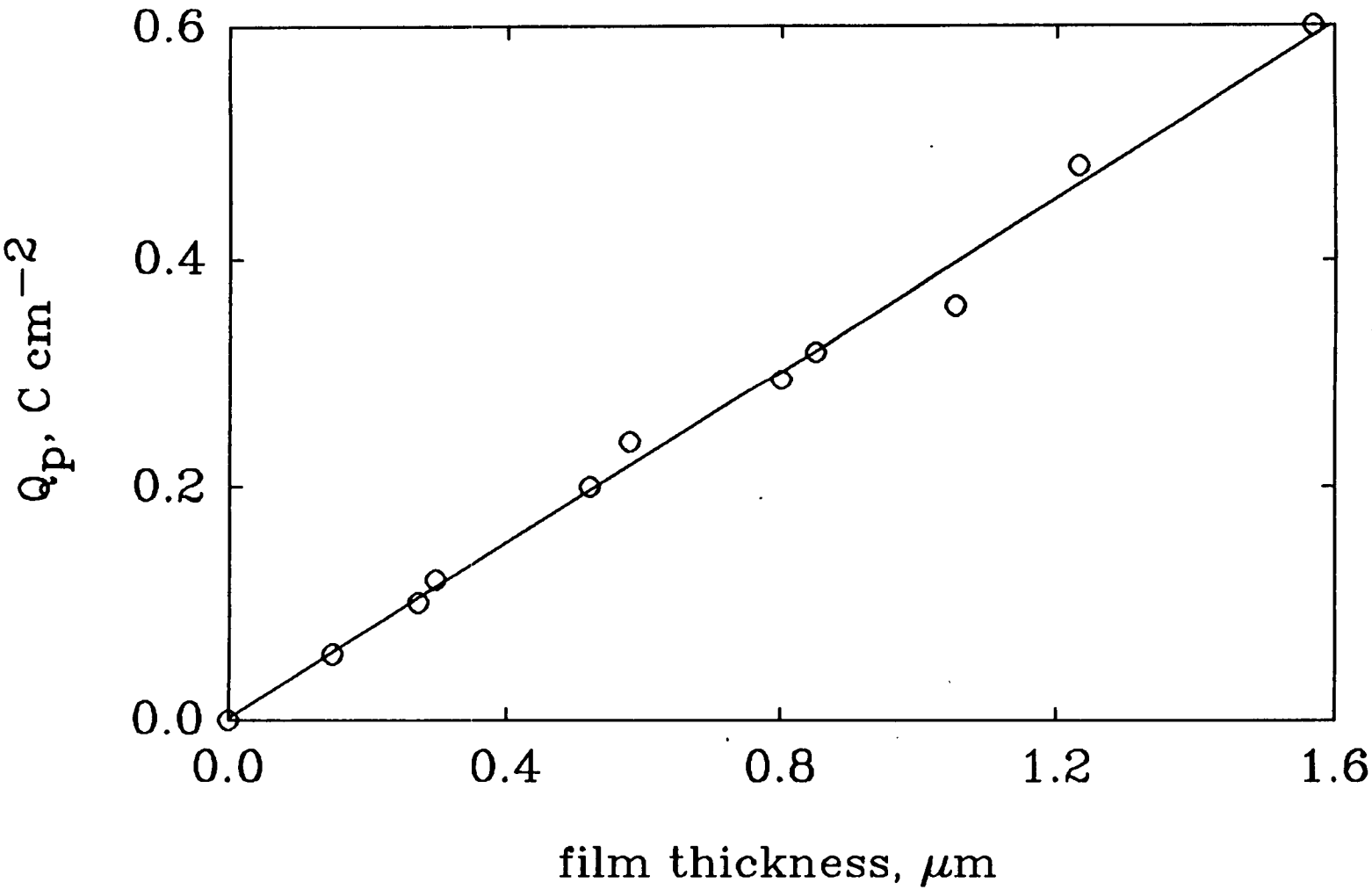

Figure 2

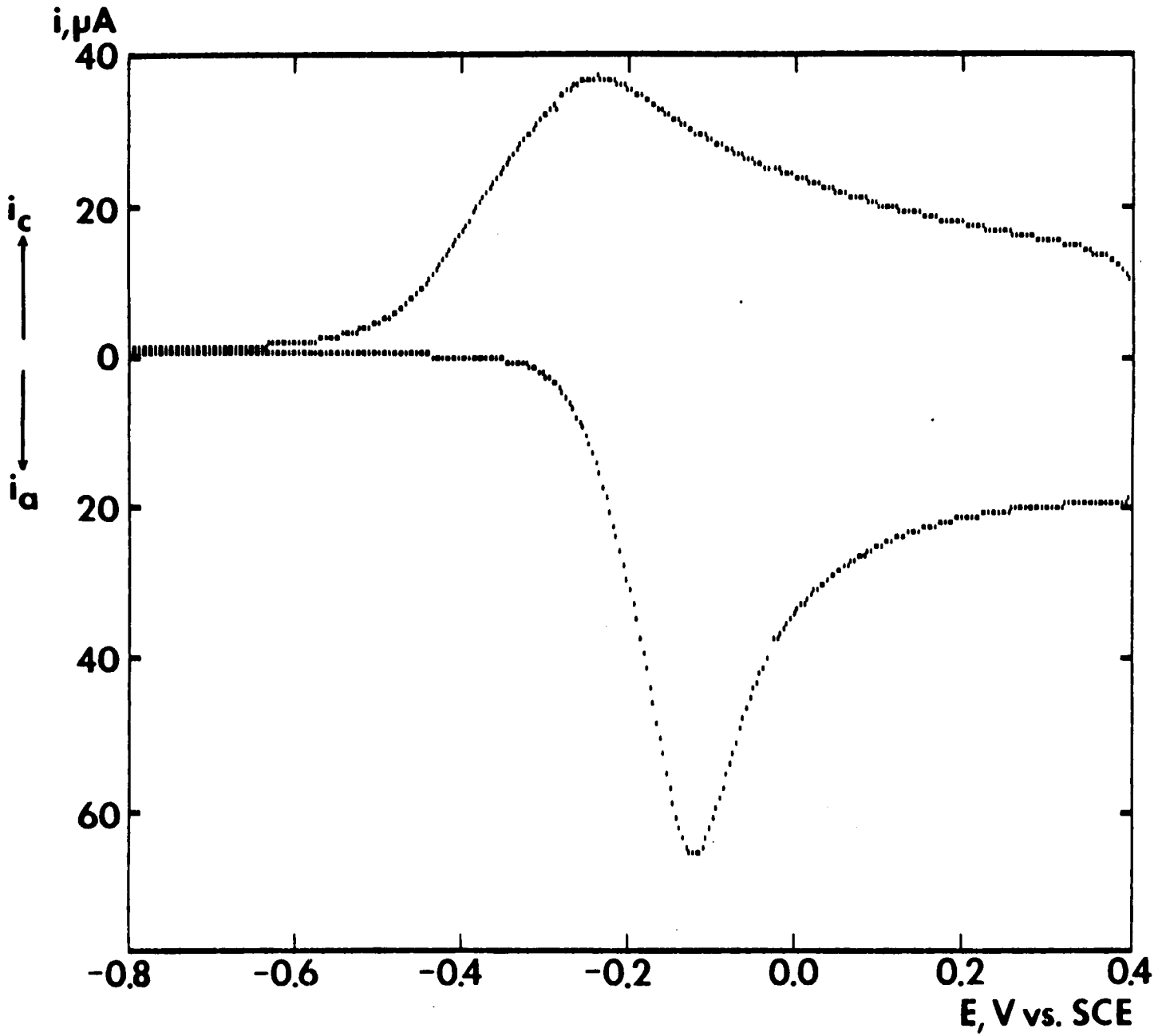

Figure 3

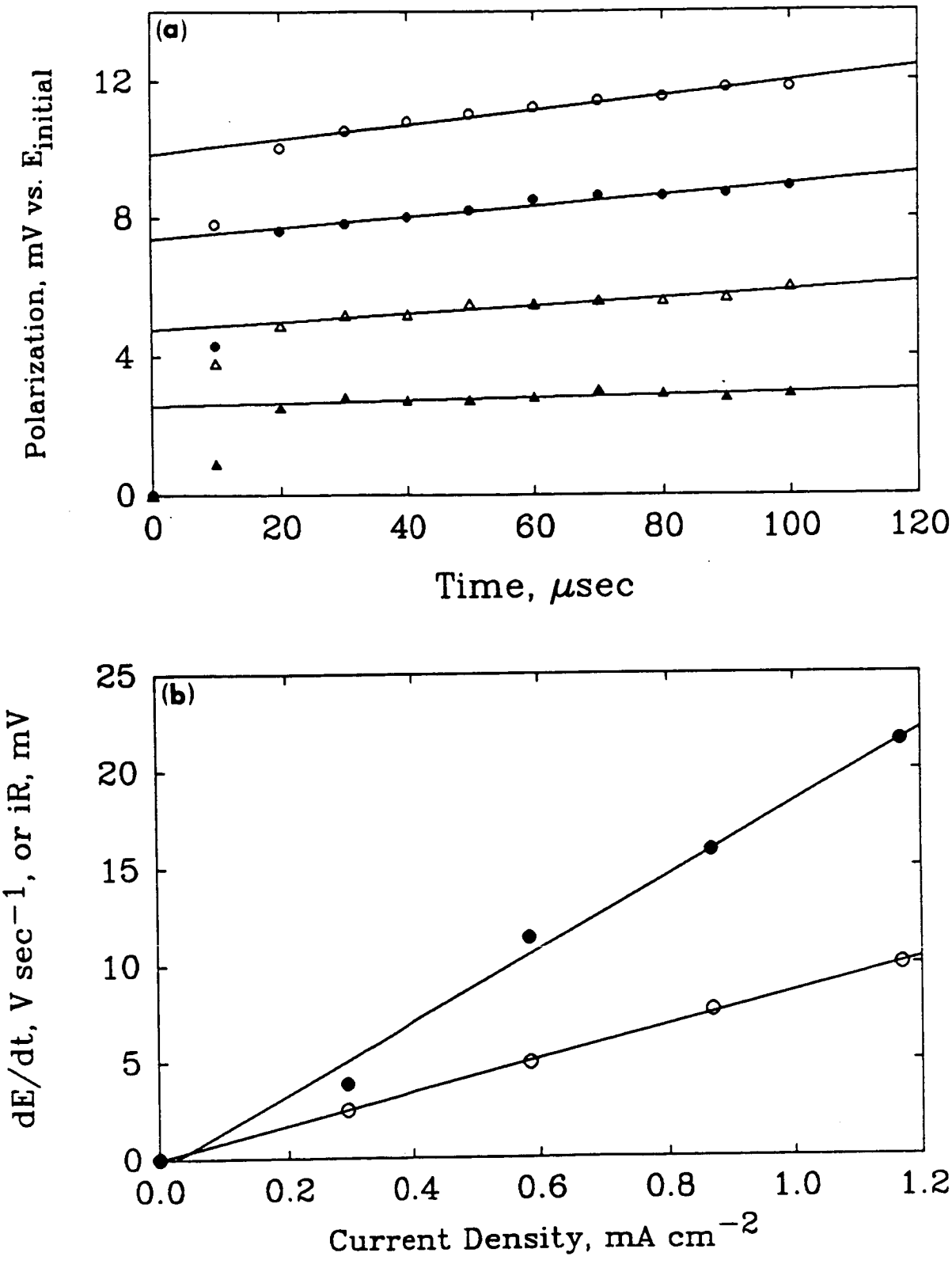
(a)
Polarization, mV vs. $E_{initial}$
12
8
4
0
0
20
40
60
80
100
120
Time, μsec
(b)
dE/dt, V sec^{-1}, or iR, mV
25
20
15
10
5
0
0.0
0.2
0.4
0.6
0.8
1.0
1.2
Current Density, mA cm^{-2}

Figure 4 (a), (b)

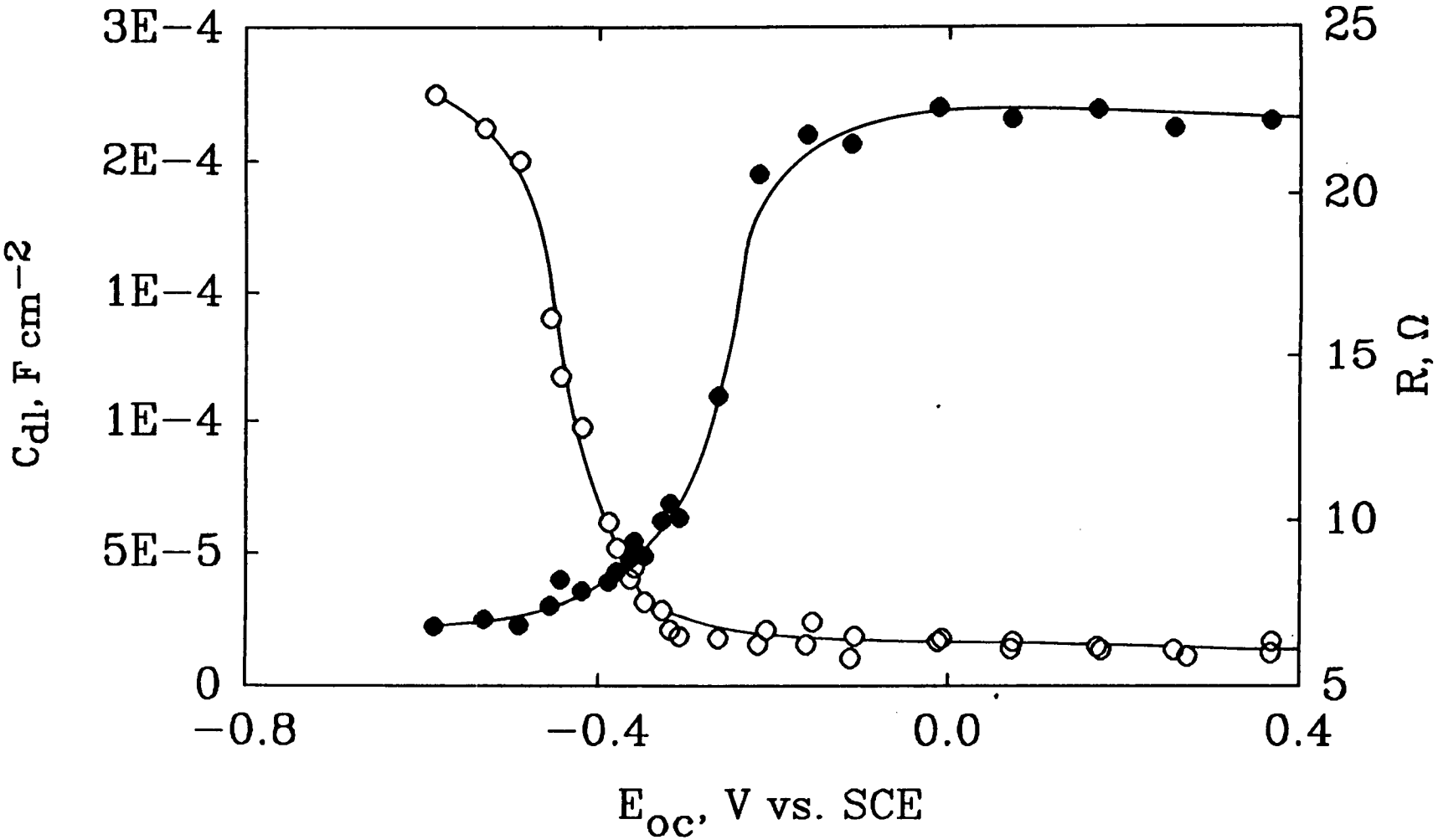
3E−4
2E−4
1E−4
1E−4
5E−5
0
25
20
15
10
5
−0.8
−0.4
0.0
0.4
C_{dl}, F cm^{-2}
R, Ω
E_{oc}, V vs. SCE

Figure 5

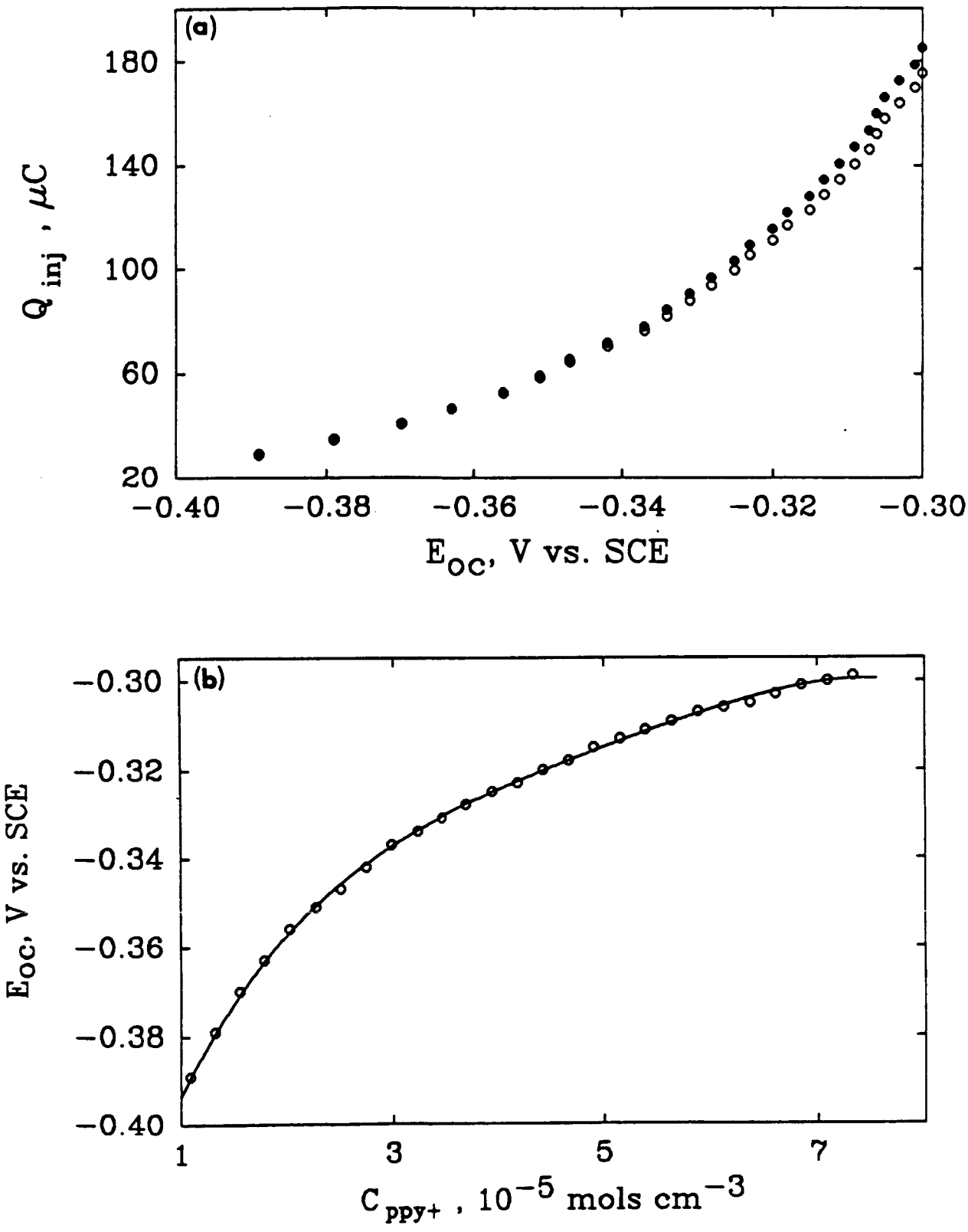
(a)
180
140
100
60
20
Q_{inj} , μC
−0.40
−0.38
−0.36
−0.34
−0.32
−0.30
E_{OC}, V vs. SCE
(b)
−0.30
−0.32
−0.34
−0.36
−0.38
−0.40
E_{OC}, V vs. SCE
1
3
5
7
C_{ppy+} , 10^{-5} mols cm^{-3}

Figure 6 (a), (b)

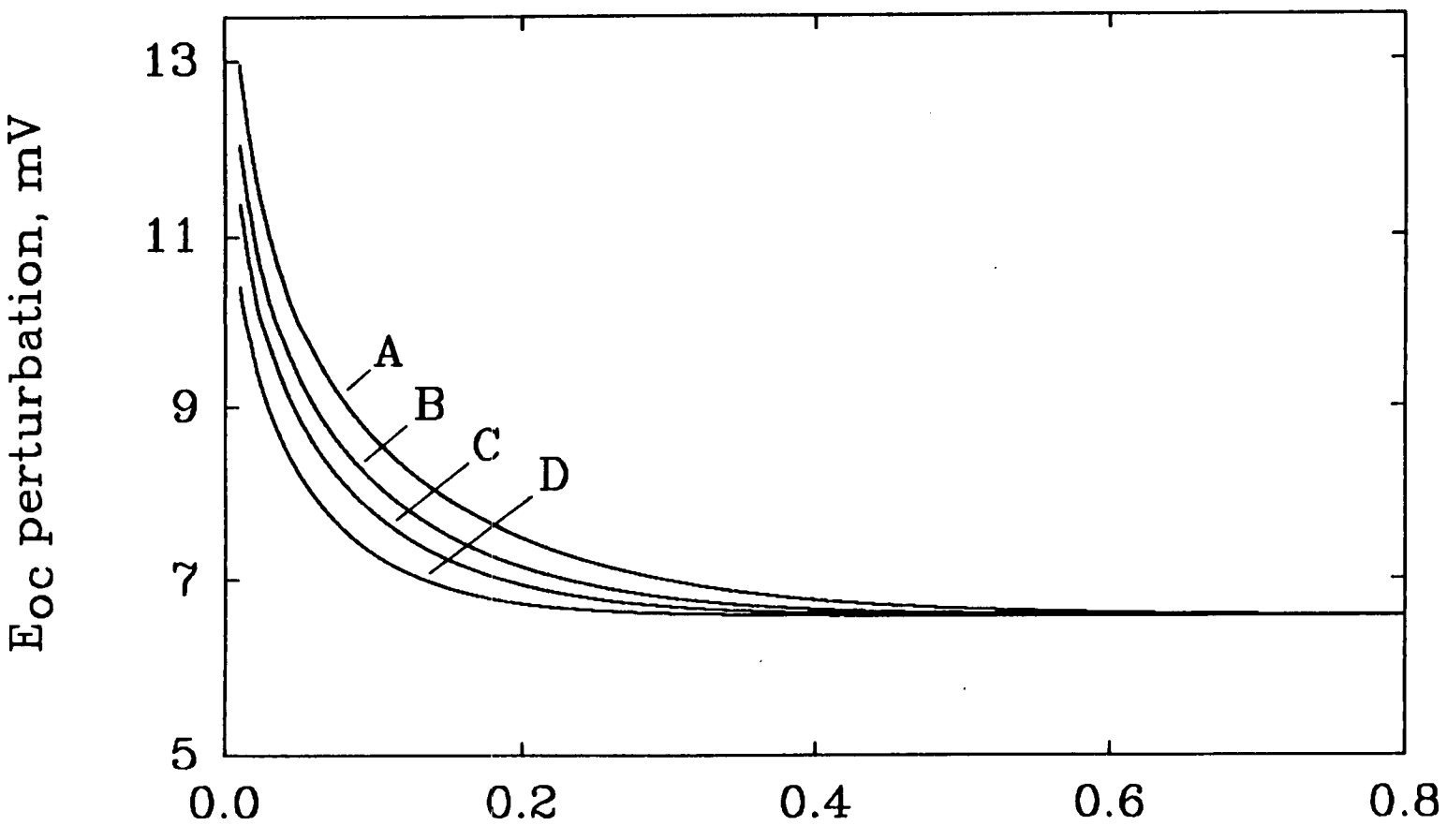

Figure 7

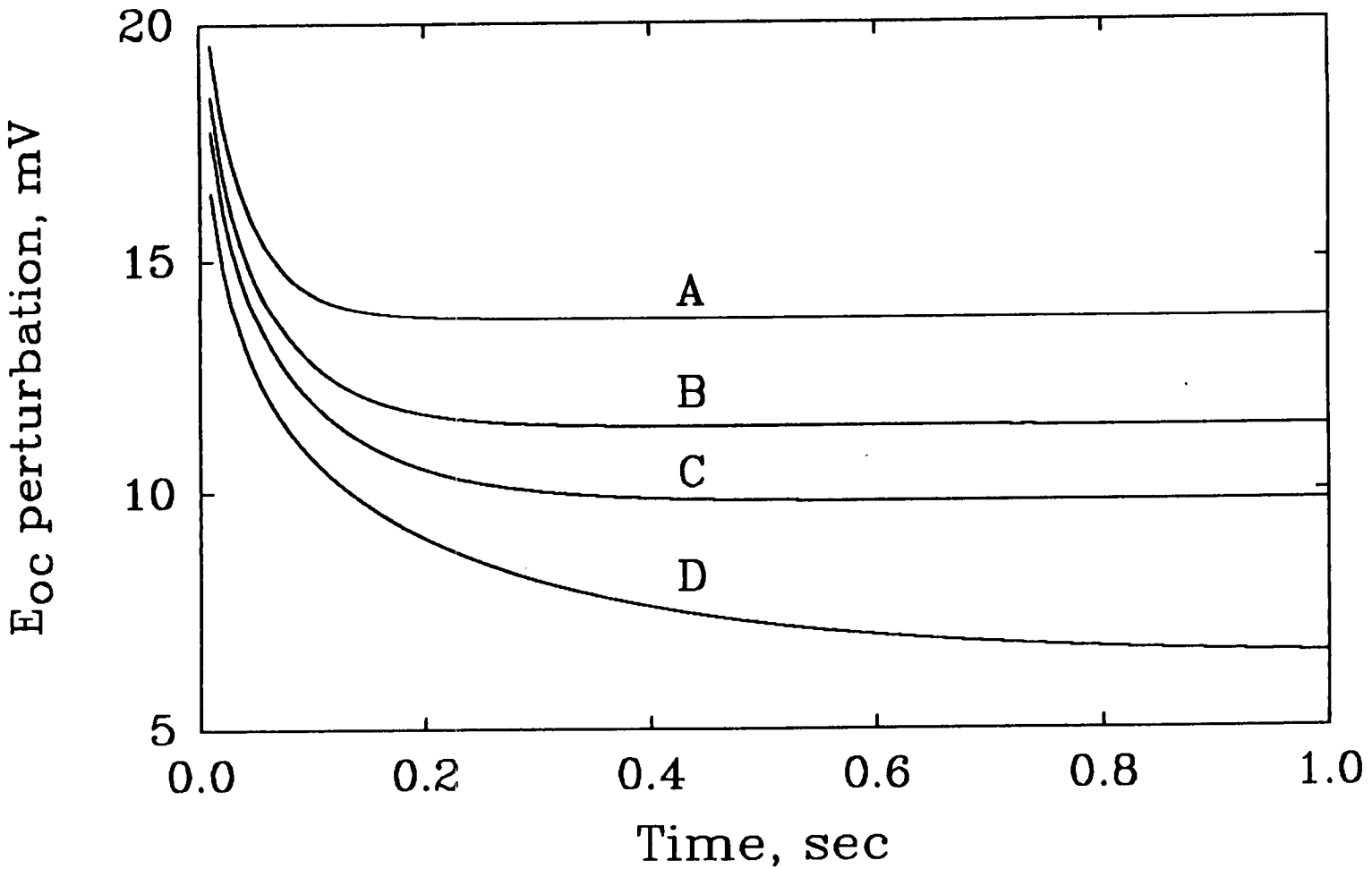

Figure 8

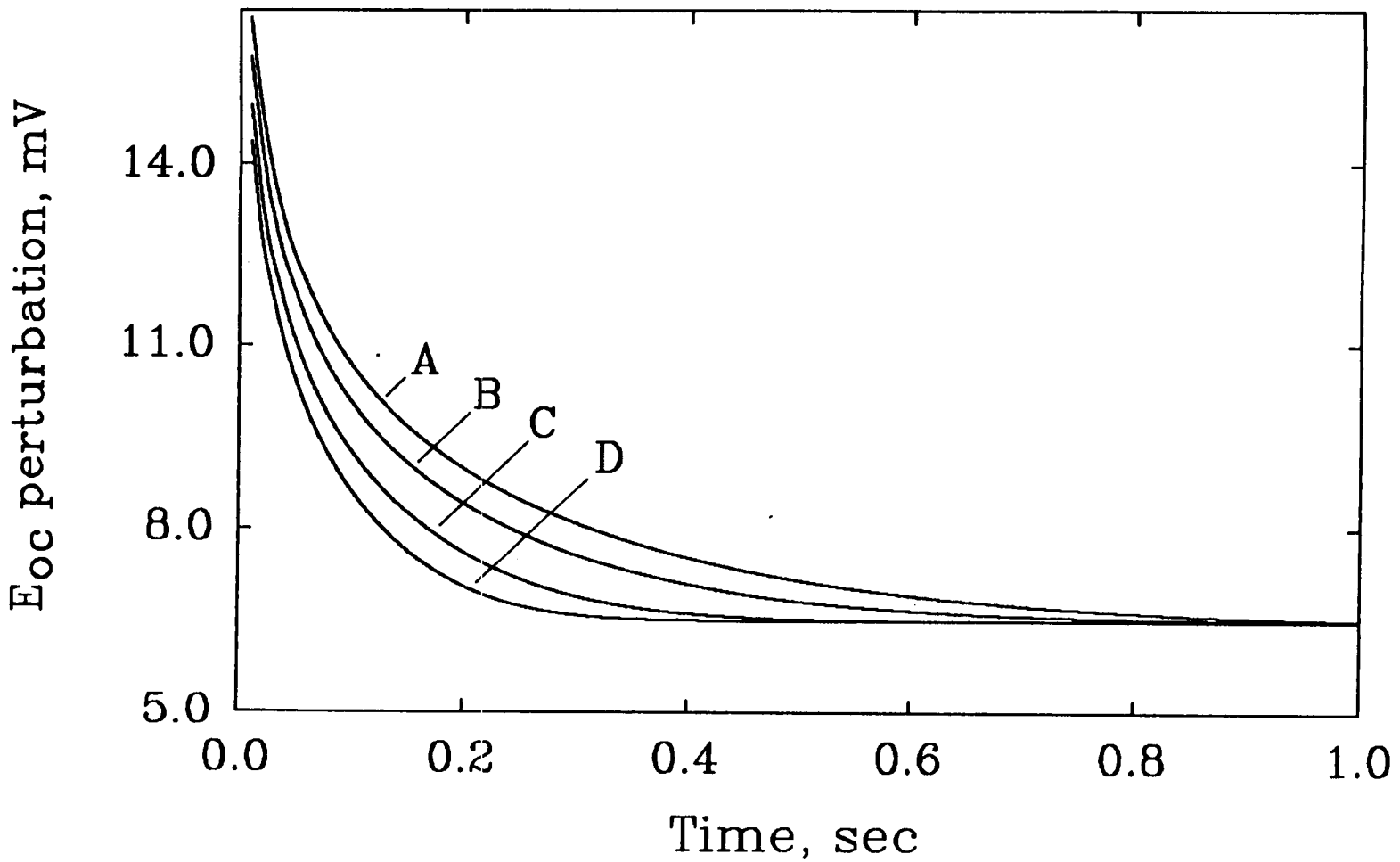
E_{oc} perturbation, mV
14.0
11.0
8.0
5.0
0.0
0.2
0.4
0.6
0.8
1.0
Time, sec
A
B
C
D

Figure 9

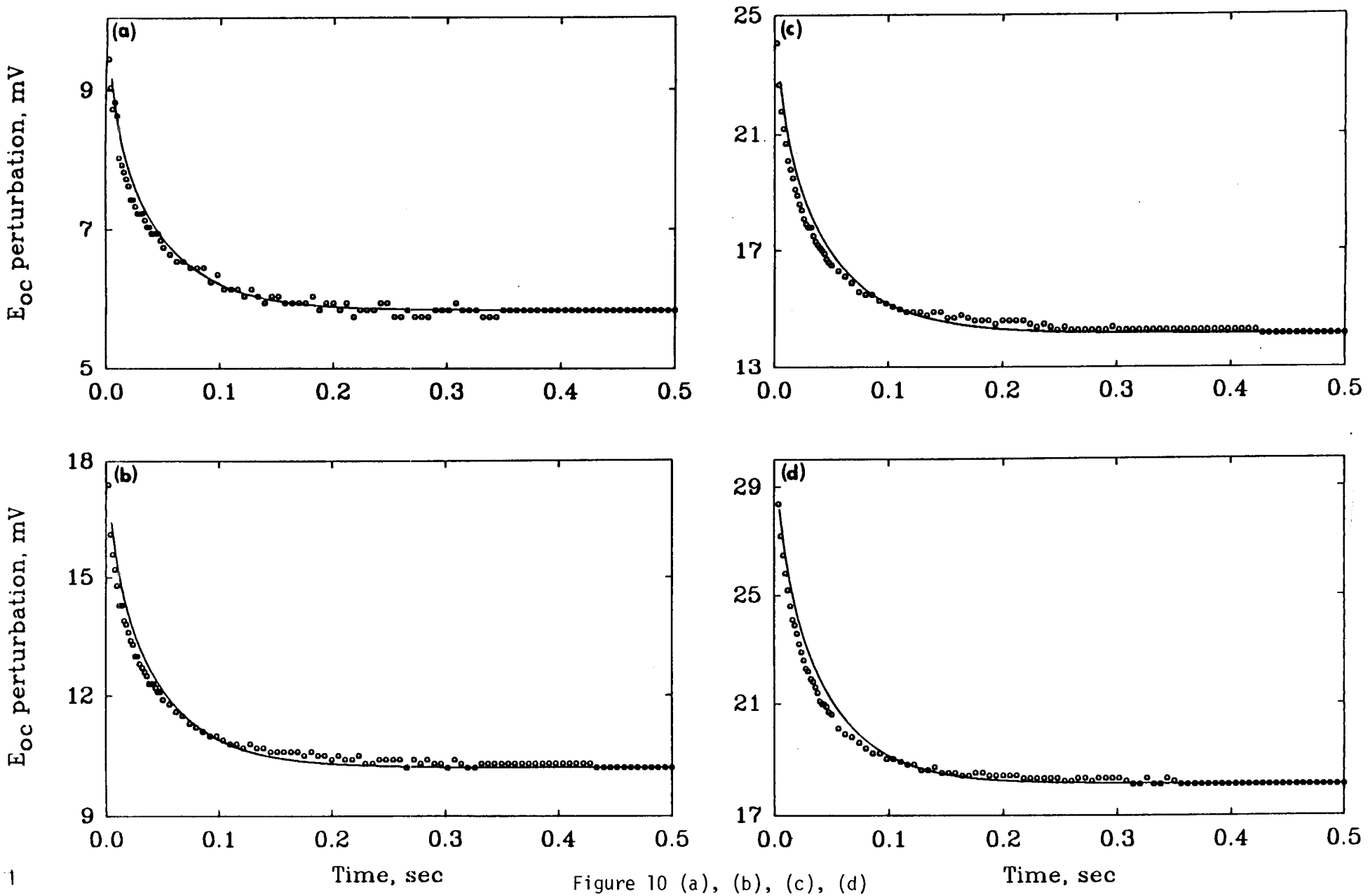

Figure 10 (a), (b), (c), (d)

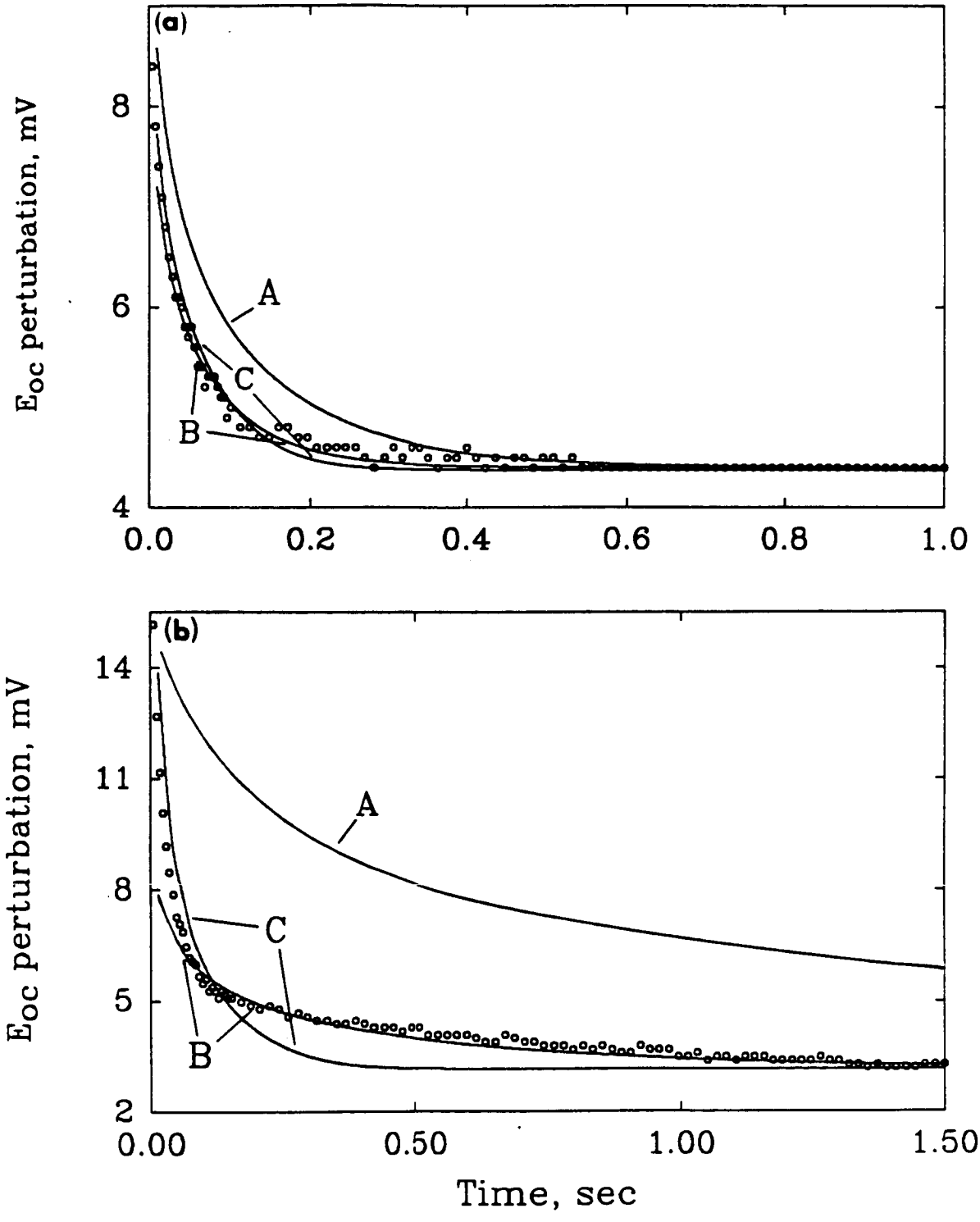
(a)
E_{oc} perturbation, mV
8
6
4
A
C
B
0.0
0.2
0.4
0.6
0.8
1.0
(b)
E_{oc} perturbation, mV
14
11
8
5
2
A
C
B
0.00
0.50
1.00
1.50
Time, sec

Figure 11 (a), (b)